

AD \_\_\_\_\_

Award Number: DAMD17-97-1-7124

TITLE: Protein-Engineered Radiometal Chelates for Immunotherapy  
of Breast Cancer

PRINCIPAL INVESTIGATOR: Jefferson Foote, Ph.D.

CONTRACTING ORGANIZATION: Fred Hutchinson Cancer Research Center  
Seattle, Washington 98104-1024

REPORT DATE: April 1999

TYPE OF REPORT: Final

PREPARED FOR: U.S. Army Medical Research and Materiel Command  
Fort Detrick, Maryland 21702-5012

DISTRIBUTION STATEMENT: Approved for Public Release;  
Distribution Unlimited

The views, opinions and/or findings contained in this report are those of the author(s) and should not be construed as an official Department of the Army position, policy or decision unless so designated by other documentation.

DTIC QUALITY INSPECTED 4

20010216 049

REPORT DOCUMENTATION PAGE			Form Approved OMB No. 0704-0188	
Public reporting burden for this collection of information is estimated to average 1 hour per response, including the time for reviewing instructions, searching existing data sources, gathering and maintaining the data needed, and completing and reviewing the collection of information. Send comments regarding this burden estimate or any other aspect of this collection of information, including suggestions for reducing this burden, to Washington Headquarters Services, Directorate for Information Operations and Reports, 1215 Jefferson Davis Highway, Suite 1204, Arlington, VA 22202-4302, and to the Office of Management and Budget, Paperwork Reduction Project (0704-0188), Washington, DC 20503.				
1. AGENCY USE ONLY (Leave blank)		2. REPORT DATE April 1999		3. REPORT TYPE AND DATES COVERED Final (1 Apr 97 - 31 Mar 99)
4. TITLE AND SUBTITLE Protein-Engineered Radiometal Chelates for Immunotherapy of Breast Cancer			5. FUNDING NUMBERS DAMD17-97-1-7124	
6. AUTHOR(S) Jefferson Foote, Ph.D.				
7. PERFORMING ORGANIZATION NAME(S) AND ADDRESS(ES) Fred Hutchison Cancer Research Center Seattle, Washington 98104-1024  E-Mail: jfoote@fhcrc.org			8. PERFORMING ORGANIZATION REPORT NUMBER	
9. SPONSORING / MONITORING AGENCY NAME(S) AND ADDRESS(ES) U.S. Army Medical Research and Materiel Command Fort Detrick, Maryland 21702-5012			10. SPONSORING / MONITORING AGENCY REPORT NUMBER	
11. SUPPLEMENTARY NOTES  This report contains colored photos				
12a. DISTRIBUTION / AVAILABILITY STATEMENT Approved for Public Release; Distribution Unlimited			12b. DISTRIBUTION CODE	
13. ABSTRACT (Maximum 200 words)  The objective of this project has been to genetically engineer a radiometal binding site in a human antibody constant region, for eventual use in tumor radioimmunotherapy. Our molecular model system was a humanized anti-lysozyme antibody Fab fragment expressed in <i>E. coli</i> . The engineered binding site, consisting of 5 point mutations in the interior of the human C $\kappa$ domain, destabilized the recombinant protein, leading to proteolysis. We attempted to address this problem by modifying the binding site design, expressing the protein within protease-negative host strains, and subcloning disulfide oxido-reductases into our expression vector, but none of these strategies resulted in a workable yield of recombinant protein. In collateral experiments, we characterized the three-dimensional structure of the anti-lysozyme.				
14. SUBJECT TERMS Breast Cancer			15. NUMBER OF PAGES 19	
			16. PRICE CODE	
17. SECURITY CLASSIFICATION OF REPORT Unclassified	18. SECURITY CLASSIFICATION OF THIS PAGE Unclassified	19. SECURITY CLASSIFICATION OF ABSTRACT Unclassified	20. LIMITATION OF ABSTRACT Unlimited	

## FOREWORD

Opinions, interpretations, conclusions and recommendations are those of the author and are not necessarily endorsed by the U.S. Army.

\_\_\_\_\_ Where copyrighted material is quoted, permission has been obtained to use such material.

\_\_\_\_\_ Where material from documents designated for limited distribution is quoted, permission has been obtained to use the material.

\_\_\_\_\_ Citations of commercial organizations and trade names in this report do not constitute an official Department of Army endorsement or approval of the products or services of these organizations.

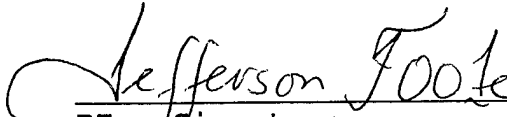
✓ In conducting research using animals, the investigator(s) adhered to the "Guide for the Care and Use of Laboratory Animals," prepared by the Committee on Care and use of Laboratory Animals of the Institute of Laboratory Resources, national Research Council (NIH Publication No. 86-23, Revised 1985).

✓ For the protection of human subjects, the investigator(s) adhered to policies of applicable Federal Law 45 CFR 46.

✓ In conducting research utilizing recombinant DNA technology, the investigator(s) adhered to current guidelines promulgated by the National Institutes of Health.

✓ In the conduct of research utilizing recombinant DNA, the investigator(s) adhered to the NIH Guidelines for Research Involving Recombinant DNA Molecules.

\_\_\_\_\_ In the conduct of research involving hazardous organisms, the investigator(s) adhered to the CDC-NIH Guide for Biosafety in Microbiological and Biomedical Laboratories.

  
PI - Signature 23 Feb 00  
Date

## Table of Contents

Front cover	1
SF 298	2
Foreword	3
Table of Contents	4
Introduction	5
Body	5
Molecular design	5
Expression in <i>E. coli</i>	6
Use of protease-negative host strains	7
Redesign of yttrium binding site	8
Construction of vector co-expressing genes that promote disulfide formation	8
Collateral experiments	9
Conclusion	9
References	9
Bibliography	10
Personnel	10
Appendices	11
Appendix I: HuLys Fab expression vector	11
Appendix II: Holmes, M. A., Buss, T. N. & Foote, J. (1998) Conformational correction mechanisms aiding antigen recognition by a humanized antibody. J. Exp. Med. 187, 479-485. (7 pp.)	

## Introduction

The isotope Yttrium-90 has decay properties ( $\beta$ -emission, path length  $<1$  cm in tissue) that would make it ideal for radioimmunotherapy. However, stable attachment of yttrium to antibodies that could target the isotope to a tumor have been problematical. The current best technology is to use a synthetic bifunctional chelator to bind the yttrium to the antibody (1). However, these synthetic molecules when bound to an immunoglobulin act as classical haptens, and can induce an immune response in patients (2). Such an immune response, directed to the radiopharmaceutical through the chelator, causes rapid inactivation and elimination of the administered therapeutic agent.

Our proposal was to genetically engineer an yttrium binding site in the constant domain of a human immunoglobulin kappa chain. The site would be located in the interior of the domain, rather than on the surface of the protein, and would be composed of charged amino acid side chains, rather than an exogenous organic molecule, hence would not be immunogenic. We chose as a model a "humanized" anti-lysozyme antibody (HuLys) that typified the type of engineered antibodies used for cancer immunotherapy. By the start of the project period, we had constructed a vector for expression of this molecule in *E. coli*.

## Body

### Molecular design

The current generation of therapeutic antibodies are all human or humanized, and of these, nearly all use kappa light chains. We therefore chose to engineer the yttrium binding site into the human kappa constant domain ( $C\kappa$ ), since such a construct, if successful, would be applicable to the widest range of therapeutic targetting vehicles.

Since there are no naturally occurring proteins containing yttrium, the preferred geometry, coordination chemistry, and preferred ligands were assessed from crystal structures of inorganic molecules in the Cambridge Structure Database. Based on a prototypic molecule, we constructed a template consisting of an yttrium ion at the center of a cube formed by eight oxygen atoms, each with a Y-O distance of 2.35-2.40Å. This template was then applied to a molecular model of the human  $C\kappa$  with the aid of a molecular graphics program (QUANTA, Molecular Simulations Inc.). We found that we could model a realistic metal binding site by changing five amino acids within the  $C\kappa$  domain and superimposing the carboxylate oxygens on the oxygen ligands of the template. In our model, shown below, six oxygen ligands are coordinated to the yttrium, all with Y-O distances between 2.24 -2.49 Å, close to the preferred bond length. With the exception of residue 136D, all side-chain conformations of mutated residues fall within acceptable limits of the Karplus rotamer library. The change 196V→A was made to provide more space for the side-chains involved in binding the metal. None of the residues that were changed is found on the exterior of the molecule or involved in interactions with the heavy chain.

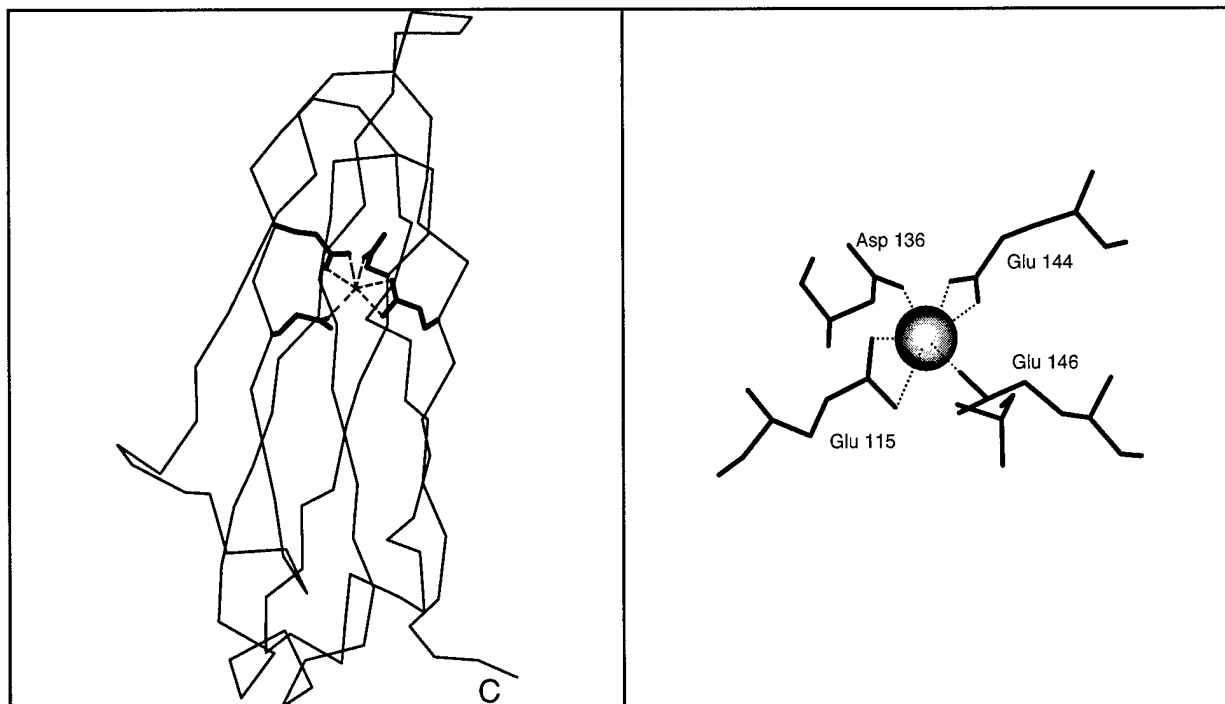
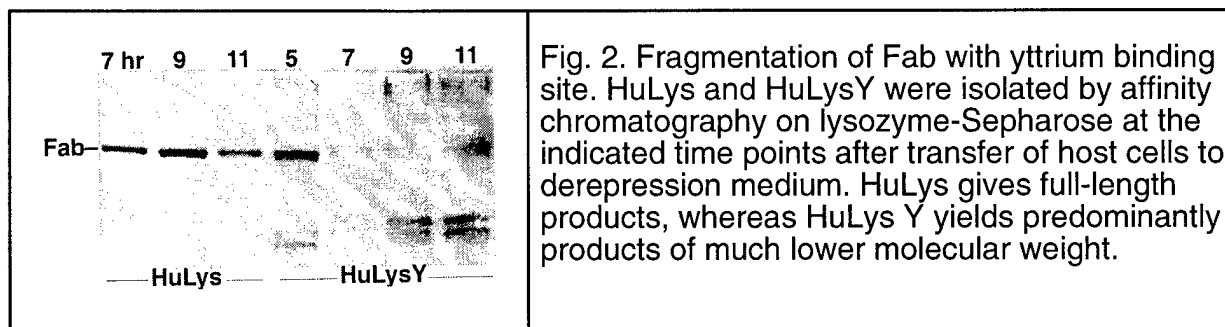


Figure 1 Model of human C $\kappa$  with engineered yttrium binding site. An  $\alpha$ -carbon trace is shown at left with Y<sup>3+</sup> and chelating side chains drawn. At right is a close view showing the Y<sup>3+</sup> ligation geometry in the model.

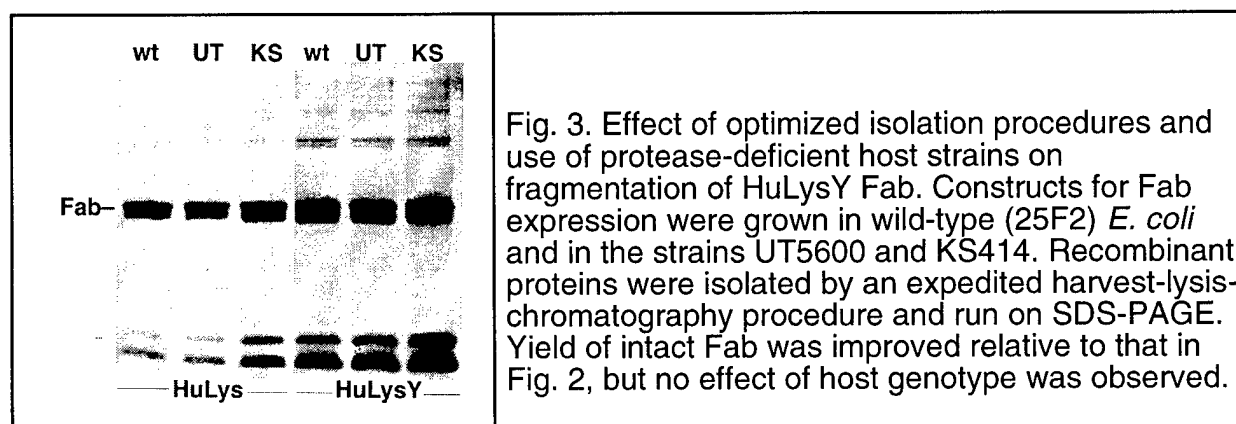
### Expression in *E. coli*

The HuLys construct was originally made as an Fv molecule (3). Genes for the HuLys Fab were cloned into an *E. coli*-based vector that uses the *phoA* promoter for the high expression of antibody Fab fragments in the periplasm (4). Mutations in the native Fab to create the internal metal binding site were introduced by means of the *dut-ung* method of oligonucleotide-directed mutagenesis (5). The sequence of the unmodified HuLys Fab expression construct is shown in Appendix I.

The construct with the yttrium binding site (HuLysY) was grown in parallel with the unmodified control in phosphate-free derepression medium, on a 200 ml scale. Cells were harvested and sonicated, and recombinant Fab were isolated on lysozyme-sepharose affinity columns. Purified proteins were analyzed by SDS-PAGE, which showed severe fragmentation of the HuLysY Fab. A representative gel is shown in Fig. 2.



Biochemical steps in the protein isolation procedure were extensively optimized, emphasizing speed, low temperature, and addition of EDTA and protease inhibitors. We exhaustively explored rapid isolation on affinity media, including peptostreptococcal protein L (6) and immobilized anti-human C $\kappa$  monoclonal antibodies 141PF11 and HP6053 (7). These modifications improved recovery of intact protein from small-scale (50 ml) cultures, but could not successfully be applied on a larger scale. A gel showing improved isolation of intact HuLysY Fab is shown in Fig. 3.



### Use of protease-negative mutant host strains

We obtained several *E. coli* strains mutant in one or more endogenous protease genes. These strains are listed in Table I. Vector constructs carrying Fab with the engineered C $\kappa$  sequence and a control with the wild-type sequence were transferred to the mutant strains, and the expression and rapid isolation procedures were applied. Surprisingly, use of the mutant strains gave no improved recovery of intact Fab. This is apparent in Fig. 3, in which expression of Fab in KS414 and UT5600 is compared to expression in the protease+ strain 25F2. The strain HM130 is mutant in all known protease genes in *E. coli*, but we were unable to isolate any recombinant protein, HuLys or HuLysY, using this host strain.

Table I. Protease-negative *E. coli* strains tested as hosts for HuLysY expression.

Strain	Relevant protease mutations	Reference
KS414	ompT degP	(8)
SG22094	lon, clpP	(9)
UT5600	ompT	(10)
HM130	degP, ptr, ompT, tsp, eda	(11)

### Redesign of the yttrium binding site

Our designed metal binding site had 4 charged amino acid side chains placed with a cubic geometry at the heart of a kappa constant region domain. This charge density obviously would destabilize the domain, but our expectation was that metal chelation would lend some stability by partially neutralizing these charges. To reduce the thermodynamically unfavorable effect of burying charges in a hydrophobic protein domain, we redesigned the metal binding site to contain 2 charged residues. Sequence modifications tested are shown in Table II. However, two alternative designs failed to increase the yield of intact protein. (Data are not shown, but do not differ substantially from Fig. 3.)

Table II. Mutated residues in the yttrium binding site – designs tested.

Construct	115	136	144	146	196
Control (wild type C $\kappa$ )	V	L	A	V	V
HuLys Y	E	D	E	E	A
HuLys Y2	E	L	E	V	A
HuLys Y3	E	L	E	V	S

### Construction of vector co-expressing genes that promote disulfide formation

Work by others has shown the importance of disulfide formation in folding of recombinant immunoglobulin fragments (12, 13). We attempted to build into our expression vector the genes for 4 enzymes used for disulfide formation in the periplasm of *E. coli*. The metabolic function of these genes and sequence references are summarized in Table III. Our presumption was that increasing the expression level of these catalysts would make immunoglobulin protein folding more rapid, hence channel more recombinant Fab down this pathway, rather than down a proteolytic pathway.



Table III. Disulfide metabolism genes incorporated into expression construct.

Gene	Function	Reference
dsbA	Oxidize protein thiols to disulfides	(14)
dsbB	Regenerate (reduce) dsbA	(15)
dsbC	Disulfide isomerase	(16, 17)
dipZ	Maintain dsbC in reduced (thiol) form	(18, 17)

We designed oligonucleotides to amplify each of these genes from *E. coli* genomic DNA. By the time the project period ended we had amplified full length dsbB and dsbC genes, and confirmed by DNA sequencing that these were the correct amplification products. We were unable to obtain correctly amplified dsbA and dipZ genes. Efforts to clone dsbB and dsbC in a pUC vector showed a surprising result, that these clones were not stable. Despite many attempts at cloning each of these genes, putative subclones isolated after transformation invariably proved to have deleted their inserts and polylinker regions. We therefore were unable to obtain data on how increasing the level of disulfide forming catalysts would affect expression of intact Fab.

#### Collateral experiments

While the foregoing work was in progress, we characterized the three-dimensional structure of the unmodified humanized anti-lysozyme, as a control in anticipation of structural studies on the yttrium-chelating version. This completed structure proved valuable in itself, and led to the sole publication from this IDEA award (19). A reprint is included as Appendix II.

#### **Conclusion**

The major obstacle in this project remains proteolytic degradation of recombinant Fab, due to the destabilizing effect of the engineered radiometal binding site. Expedited procedures for biochemical isolation of recombinant Fab are improved the yield of intact protein, but not to a decisive level. Use of host strains with single or double protease mutations did not improve expression. Building the binding site sequentially, one amino acid residue at a time, was not a successful strategy for remediating the observed protein instability. This IDEA project was therefore a failure. A new approach, probably employing combinatorial mutagenesis and selection methods, is necessary to genetically build an yttrium binding site in an immunoglobulin constant domain.

#### **References**

1. Deshpande, S. V., DeNardo, S. J., Kukis, D. L., Moi, M. K., McCall, M. J., DeNardo, G. L. & Meares, C. F. (1990) Yttrium-90-labeled monoclonal antibody for therapy: labeling by a new macrocyclic bifunctional chelating agent. *J. Nucl. Med.* 31, 473-479.
2. Kosmas, C., Maraveyas, A., Gooden, C. S., Snook, D. & Epenetos, A. A. (1995) Anti-chelate antibodies after intraperitoneal yttrium-90-labeled monoclonal antibody immunoconjugates for ovarian cancer therapy. *J. Nucl. Med.* 36, 746-753.
3. Riechmann, L., Foote, J. & Winter, G. (1988) Expression of an antibody Fv fragment in myeloma cells. *J. Mol. Biol.* 203, 825-828.
4. Carter, P., Kelley, R. F., Rodrigues, M. L., Snedecor, B., Covarrubias, M., Velligan, M. D., Wong, W. L. T., Rowland, A. M., Kotts, C. E., Carver, M. E., Yang, M., Bourell, J. H., Shepard, H. M. &

- Henner, D. (1992) High level *Escherichia coli* expression and production of a bivalent humanized antibody fragment. *Bio/Technology* 10, 163-167.
5. Kunkel, T. A. (1985) Rapid and efficient site-specific mutagenesis without phenotypic selection. *Proc. Natl. Acad. Sci. USA* 82, 488 -492.
  6. Ståhl, S., Nygren, P.-Å., Sjölander, A. & Uhlén, M. (1993) Engineered bacterial receptors in immunology. *Curr. Opin. Immunol.* 5, 272-277.
  7. Reimer, C. B., Phillips, D. J., Aloisio, C. H., Moore, D. D., Galland, G. G., Wells, T. W., Black, C. M. & McDougal, J. S. (1984) Evaluation of thirty-one mouse monoclonal antibodies to human IgG epitopes. *Hybridoma* 3, 263-275.
  8. Strauch, K. L., Johnson, K. & Beckwith, J. (1989) Characterization of degP, a gene required for proteolysis in the cell envelope and essential for growth of *Escherichia coli* at high temperature. *J. Bacteriol.* 171, 2689-2696.
  9. Maurizi, M. R., Clark, W. P., Katayama, Y., Rudikoff, S., Pumphrey, J., Bowers, B. & Gottesman, S. (1990) Sequence and structure of Clp P, the proteolytic component of the ATP-dependent Clp protease of *Escherichia coli*. *J. Biol. Chem.* 265, 12536-12545.
  10. Earhart, C. F., Lundrigan, M., Pickett, C. L. & Pierce, J. R. (1979) *Escherichia coli* K-12 mutants that lack major outer membrane protein a. *FEMS Microbiol. Lett.* 6, 277-280.
  11. Meerman, H. J. & Georgiou, G. (1994) Construction and characterization of a set of *E. coli* strains deficient in all known loci affecting the proteolytic stability of secreted recombinant proteins. *Bio/Technology* 12, 1107-1110.
  12. Glockshuber, R., Malia, M., Pfitzinger, I. & Plückthun, A. (1990) A comparison of strategies to stabilize immunoglobulin Fv fragments. *Biochemistry* 29, 1362-1367.
  13. Wulfig, C. & Plückthun, A. (1994) Correctly folded T-cell receptor fragments in the periplasm of *Escherichia coli*. Influence of folding catalysts. *J. Mol. Biol.* 242, 655-669.
  14. Bardwell, J. C., McGovern, K. & Beckwith, J. (1991) Identification of a protein required for disulfide bond formation in vivo. *Cell* 67, 581-589.
  15. Missiakas, D., Georgopoulos, C. & Raina, S. (1993) Identification and characterization of the *Escherichia coli* gene dsbB, whose product is involved in the formation of disulfide bonds in vivo. *Proc. Natl. Acad. Sci. USA* 90, 7084-7088.
  16. Missiakas, D., Georgopoulos, C. & Raina, S. (1994) The *Escherichia coli* dsbC (xprA) gene encodes a periplasmic protein involved in disulfide bond formation. *EMBO J.* 13, 2013-2020.
  17. Rietsch, A., Belin, D., Martin, N. & Beckwith, J. (1996) An in vivo pathway for disulfide bond isomerization in *Escherichia coli*. *Proc. Natl. Acad. Sci. USA* 93, 13048-13053.
  18. Missiakas, D., Schwager, F. & Raina, S. (1995) Identification and characterization of a new disulfide isomerase-like protein (DsbD) in *Escherichia coli*. *EMBO J.* 14, 3415-3424.
  19. Holmes, M. A., Buss, T. N. & Foote, J. (1998) Conformational correction mechanisms aiding antigen recognition by a humanized antibody. *J. Exp. Med.* 187, 479-485.

## Bibliography

Holmes, M. A., Buss, T. N. & Foote, J. (1998) Conformational correction mechanisms aiding antigen recognition by a humanized antibody. *J. Exp. Med.* 187, 479-485.

## Personnel

Jefferson Foote  
Margaret A. Holmes  
Timothy N. Buss  
Emily Johnson

## Appendix I: HuLys Fab expression vector

```

                20                40                60                80
GAATTCAACTTCTCCATCT TGGATAAGGAAATACAGAC ATGAAAAATCTCATTCGTGA GTTGTATTATTAAGGTTGCC
100                120                140                160
AAAAAGAAGAAGAGTGAAT GAACTGTGTGCGCAGGTAGA AGGTTTGGAGATTATCGTCA CTGCAATGCTTCGCAATATG
180                200                220                240
GCGCAAAATGACCAACAGCG GTTGATTGATCAGGTAGAGG GGGCGCTGTACGAGGTAAAG CCGATGCCAGCATTCCTGA
260                280                300                320
CGACGATACGGAGCTGCTGC GCGATTACGTAAAGAAGTTA TTGAAGCATCCTCGTCAGTA AAAAGTTAATCTTTTCAACA

phoB_binding_box      phoA_promoter
|                      |
340                360                380                400
GCTGTCATAAAGTTGTACG GCGAGACTTATAGTCGCTT TGTTTTTATTTTTTAAATGTA TTTGTAAGTAGAATTGAGC
                >rbs
420                440                460                480
TCGGTACCGGGGATCCTCT AGAGGTTGAGGTGATTTTAT GAAAAAGAATATCGCATTTT TTTCTGCATCTATGTTCTG
                M K K N I A F L L A S M F V>
                _____STII SIGNAL SEQUENCE_____>

500                520                540                560
TTTCTATTGCTACAAACGC GTACGCTGACATCCAGATGA CCCAGAGCCCAAGCAGCGCTG AGCGCCAGCGTGGGTGACAG
F S I A T N A Y A D I Q M T Q S P S S L S A S V G D R>
                _____STII SIGNAL SEQUENCE_____HULYS VL_____>

580                600                620                640
AGTGACCATCACTGTAGAG CCAGCGGTAAACATCCACAAC TACCTGGCTTGTACCAGCA GAAGCCAGGTAAAGCTCCAA
V T I T C R A S G N I H N Y L A W Y Q Q K P G K A P>
                _____HULYS VL_____>

660                680                700                720
AGCTGTGATCTACTACACC ACCACCCCTGGCTGACGGTGT GCGAAGCAGATTACAGCGGTA GCGGTAGCGGTACCGACTTC
K L L I Y Y T T T L A D G V P S R F S G S G S G T D F>
                _____HULYS VL_____>

740                760                780                800
ACCTTCACCATCAGCAGCT CCAGCCAGAGGACATGCGCA CCTACTACTGCCAGCACTTC TGGAGCACCCCAAGGACGTT
T F T I S S L Q P E D I A T Y Y C Q H F W S T P R T F>
                _____p_____HULYS VL_____p_____>

820                840                860                880
CGGCCAAGGACCAAGGTGG AAATCAAACGTGGAACGTGT GCTGCACCATCTGTCTTCAT CTTCCCGCCATCTGATGAGC
G Q G T K V E I K R> R T V A A P S V F I F P P S D E>
                _____HULYS VL_____>C-KAPPA_____>

900                920                940                960
AGTTGAAATCTGGAAGTCC TCTGTGTGTGCTGCTGAA TAACTTCTATCCAGAGAGG CCAAAGTACAGTGAAGGTG
Q L K S G T A S V V C L L N N F Y P R E A K V Q W K V>
                _____C-KAPPA_____>

980                1000                1020                1040
GATAACGCCCTCCAATGGG TAACTCCAGGAGGTGTCA CAGAGCAGGACAGCAAGGAC AGCACTACAGCCCTCAGCAG
D N A L Q S G N S Q E S V T E Q D S K D S T Y S L S S>
                _____C-KAPPA_____>

1060                1080                1100                1120
CACCTGACGCTGAGCAAAG CAGACTACGAGAAACACAAA GTCTACGCTGCGAAGTCAC CCATCAGGCGCTGAGCTGCG
T L T L S K A D Y E K H K V Y A C E V T H Q G L S S>
                _____C-KAPPA_____>

1140                1160                1180                1200
CCGTCACAAAGAGCTTCAAC AGGGGAGAGTGTTAAGCTGA TCCTCTACGCCGGACGCATC GTGGCCCTAGTACGCAAGTT
P V T K S F N R G E C>
                _____C-KAPPA_____>

```



# Conformational Correction Mechanisms Aiding Antigen Recognition by a Humanized Antibody

By Margaret A. Holmes, Timothy N. Buss, and Jefferson Foote

*From the Division of Molecular Medicine, Fred Hutchinson Cancer Research Center, Seattle, Washington 98109-1024*

## Summary

The crystal structure of the complex between hen egg lysozyme and the Fv fragment of a humanized antilysozyme antibody was determined to 2.7-Å resolution. The structure of the antigen combining site in the complex is nearly identical to that of the complexed form of the parent mouse antibody, D1.3. In contrast, the combining sites of the unliganded mouse and humanized antilysozymes show moderate conformational differences. This disparity suggests that a conformational readjustment process linked to antigen binding reverses adverse conformations in the complementarity determining regions that had been introduced by engineering these segments next to human framework regions in the humanized antibody.

Humanized antibodies were designed to limit the response of the human immune system to rodent monoclonal antibodies used in therapy of human disease (1). They represented an advance over chimeric antibodies (2–4), which were engineered with murine immunoglobulin variable domains and human constant domains, in that the foreign content of humanized variable regions was substantially reduced. This was achieved by combining the short, hypervariable complementarity determining regions (CDRs)<sup>1</sup> of a murine antibody, which fold to form an antigen combining site of unique structure, with human variable domain framework regions, which appear to be conserved in sequence throughout all races (5–9). The resulting molecule has the same specificity as the murine antibody, but substitution of human sequences confers a much longer in vivo lifetime and nearly eliminates immunogenic side effects (10).

Framework and CDR segments can be identified from sequence information alone, since they are defined by homology rather than structure (11, 12). At the three-dimensional level, however, the two sets of residues are in intimate contact and mutually influence each other's conformation (13, 14). Human framework residues can alter the conformation of transposed mouse CDRs and thereby disrupt antigen binding. Since human and mouse framework regions differ by upwards of 50 out of 170 residues (15), the potential for this sort of disruption is high. Nevertheless, humanizing by

grafting mouse CDRs onto human frameworks usually transfers antigenic specificity, though sometimes additional framework mutations are required to put antigen affinity on a par with the starting mouse antibody (13).

In this report, we describe intrinsic aspects of immunoglobulin structure that may partly account for the ease with which CDRs and framework regions from different animal species and unrelated antigenic specificities may be combined to give a functional molecule. We have determined the crystal structure of the complex between hen egg white lysozyme and the immunoglobulin heavy and light chain variable domains (Fv) of a humanized version of the mouse antilysozyme D1.3 (HuLys). This is the first reported structure of a complex of antigen with a humanized antibody, and completes a family of crystallographically determined component structures. D1.3 was previously determined in the free form and complexed with lysozyme, both at 1.8-Å resolution (16, 17). HuLys was determined in the unliganded form at 2.9-Å resolution (14). The human immunoglobulins NEW and REI, from which the HuLys heavy and light chain framework regions were taken, respectively, have previously been determined in their unliganded form, both at 2.0-Å resolution (18–20). The availability of mouse, human, and antigen complex structures for reference has now allowed us to identify conformational differences in the humanized Fv that result from protein engineering and ligand binding.

## Materials and Methods

**Protein Expression.** The HuLys protein used in this study was a high affinity form with variable domain sequences identical to those published previously (21). This molecule was expressed as

<sup>1</sup>Abbreviations used in this paper: Cα, alpha carbon; CDR, complementarity determining region; Fv, dimer of immunoglobulin heavy and light chain variable domains; rms, root mean square.

**Table 1.** Data Collection

Parameter	Data set 1 value	Data set 2 value
Resolution	Å	Å
Entire data set	50.0–3.5	50.0–2.7
Last shell	3.56–3.0	2.75–2.70
Reflections		
Total	73,185	120,820
Unique	9,493	22,379
Completeness	%	%
Entire data set	85.1	93.2
Last shell	76.3	73.5
R value*		
Entire data set	0.078	0.075
Last shell	0.226	0.452
Average I/ $\sigma_1$	10.3	9.6

$$^*R = \frac{\sum_{hkl} \sum_i |I_{i,hkl} - \langle I_{hkl} \rangle|}{\sum_{hkl} \sum_i I_{i,hkl}}$$

an Fv fragment in the *Escherichia coli* strain 25F2, using the vector pAK19 (22). In brief, 15 liters of defined medium (23) supplemented with 0.15% casamino acids, 1% glucose, and 20  $\mu$ g/ml tetracycline was inoculated with 400 ml of a starter culture (absorbance at 600 nm 1.5–2) and grown in a fermentor (New Brunswick Scientific MPP, Edison, NJ) for 20 h at 37°C. Cells were harvested by centrifugation and subjected to osmotic shock to release periplasmic proteins (24). The periplasmic fraction was clarified by centrifugation (30 min at 14,500 g) and passed through a lysozyme–Sepharose column. After extensive washes with PBS and high salt buffer (500 mM NaCl, 50 mM Tris, pH 8.5), the Fv was eluted with 50 mM diethylamine.

**Crystallization.** The purified Fv was complexed with lysozyme and crystallized from phosphate buffer. Lysozyme (three times crystallized) was purchased from Sigma Chemical Co. (St. Louis, MO) and dissolved in PBS. HuLys–lysozyme complex was prepared by mixing the two in equimolar proportions, letting the solution sit for 30 min, and diluting to 10  $\mu$ g/ml with PBS. There was immediate slight cloudiness upon mixing; the solution was spun in a bench-top centrifuge before setting up crystallizations. Crystallization was by vapor diffusion; both hanging drops and sitting drops in microbridges were used. Protein concentration was 7 or 10 mg/ml. The reservoir was 1.6 or 1.7 M phosphate (made by mixing equal volumes of  $K_2HPO_4$  and  $NaH_2PO_4$ ), and 0.1 M Hepes, pH 6.5. Equal volumes of protein and reservoir solutions were mixed to make the drop.

**Data Collection.** Two x-ray diffraction data sets were collected to 2.9-Å resolution and 2.7-Å resolution, each from a single crystal at 4°C, using an r-axis detector. The two data sets were processed (Table 1) with DENZO and SCALEPACK (25). The lower resolution data set, truncated to 3.5 Å, was used initially for determining the molecular replacement solution. Refinement was carried out when the higher resolution data set became available.

**Molecular Replacement Solution.** A search model for molecular replacement was constructed by superposing molecule 2 of uncomplexed HuLys (14), the molecule whose CDRs are less affected by crystal packing, upon the murine complexed structure and combining the HuLys and lysozyme structures. Molecular re-

**Table 2.** Refinement

Parameter	Value
Resolution	10.0–2.7 Å
Reflections	
Total (F > 2 $\sigma$ )	18,822
Working set	16,927
Test set	1,895
Atoms	5,490
R value	
Working	0.208
Free	0.297
rms deviation from ideality	
Bond lengths	0.014 Å
Bond angles	1.8°
PROCHECK analysis, percent residues in:	
Most favored regions	79.3
Additional allowed regions	19.2
Generously allowed regions	1.2
Disallowed regions	0.3

placement was carried out using the program AMoRe (26) with the 3.5-Å resolution data set. The space group was determined to be P4<sub>1</sub>2<sub>1</sub>2 from the four possibilities P4<sub>x</sub>2<sub>1</sub>2, x = 0, 1, 2, 3, by solution of the translation function. (There were no 00l reflections in the data set.) The unit cell dimensions were a = b = 97.7 Å, and c = 174.9 Å. After refinement of the translation functions for the two molecules in the asymmetric unit, the correlation coefficient was 0.63 and the R value was 0.38 (15–3.5 Å).

**Crystallographic Refinement.** The 2.7-Å resolution data set was partitioned by X-PLOR (27) into two sets, one for refinement and calculation of the working R value, and the other for calculation of the free R value (28, 29). A rigid-body refinement was performed at 3.5-Å resolution using X-PLOR, first with each complex as a rigid body, and then with each chain as a rigid body. The refinement resulted in a drop of both working R and free R from 0.46 to 0.32 (10–3.5 Å). Alternating rounds of positional and individual B value refinement, using both X-PLOR and TNT (30), and model building, using QUANTA (Molecular Simulations, Inc., Burlington, MA), were performed (Table 2). No solvent molecules were included in the model. The values for working R and free R dropped from 0.35 to 0.21 and from 0.34 to 0.30, respectively (10–2.7 Å). A PROCHECK analysis (31) of the structure showed no residues in disallowed regions of a Ramachandran plot except for residue L51 of both molecules. This is also seen in the uncomplexed HuLys and REI and many other Fab structures. The residue is in a  $\gamma$ -turn conformation (32). Residue numbering follows the Kabat system (15). In this paper we precede each residue number with a chain designator, e.g., L51 for light chain residue 51.

## Results

**Antigen–Antibody Interaction.** The most striking feature of the structure is apparent when the antigen-contacting residues in the mouse and humanized Fv–lysozyme com-

plexes are compared to the same residues seen in the free Fv structures. The unliganded structures are shown superposed in Fig. 1 A. A multitude of conformational differences are observed between the unliganded mouse and humanized combining sites. In contrast, the antigen-contacting residues in the HuLys and D1.3 complexes have virtually identical conformations (Fig. 1 B). Although these superpositions were calculated using only alpha carbon (C $\alpha$ ) atoms of the polypeptide chains, it is clear that the side chain conformations are also nearly identical in the complexed structures.

Several of the differences between complexed and uncomplexed forms in Fig. 1 occur not because of antigen binding, but because the antigen-binding residues in the uncomplexed Fv are involved in crystal packing interactions. The largest shift amongst antigen-contacting residues of the murine Fv (0.69–1.06 Å) occurs for heavy chain residues H96–H98 (16), and probably arises from contacts with symmetry-related molecules in the uncomplexed Fv. A comparison of the uncomplexed and complexed forms of HuLys Fv shows that the largest shift amongst antigen-contacting residues occurs for residue L93; the C $\alpha$ –C $\alpha$  distances after CDR superposition are 1.20 and 1.31 Å for molecules 1 and 2, respectively, versus molecule 2 of the uncomplexed Fv structure. This large shift is not seen upon examination of the D1.3 structures, possibly because in uncomplexed D1.3, this residue may be held in a complexed-like conformation due to crystal packing interactions. All other shifts in antigen-contacting residues are less than twice the root mean square (rms) distance for the superposition of all six CDRs.

The rearrangements accompanying lysozyme binding represent a broader effect than symmetry-related intermolecular contacts alone can account for. Quantitative evidence that the CDRs of the liganded forms of HuLys and D1.3 are more structurally similar than in the free Fv molecules is presented in Table 3. The rms differences in position of C $\alpha$  atoms in the mouse and humanized CDRs, which comprise 56 residues in each molecule, is 0.37 Å when the Fv–lysozyme complexes are compared, versus 0.63 Å comparing the CDRs in the free Fvs (33). The liganded CDRs are closer in structure than any other residue subset in Table 1. In addition, the binding of lysozyme by HuLys causes the CDRs to more closely resemble the unbound D1.3 CDRs. Even superposition of the lysozyme molecule in the HuLys complex onto the lysozyme molecule in the D1.3 complex gives a rms distance one fourth larger than for the corresponding CDRs. Lysozyme itself forms crystal packing interactions that differ in the mouse and HuLys complexes, which give rise to some of the differences.

Contacts between HuLys and lysozyme were identified using the program PAIRS (34). An analysis of these contacts is given in Table 4. Only direct protein–protein hydrogen bonds are considered, as we have not included water molecules in the HuLys structure due to its lower resolution. Solvent molecules do in fact contribute greatly to the stabilization of the complex, as was seen in the higher reso-

lution D1.3 complex structure (35). The hydrogen bond distances in the D1.3 and HuLys complexes are similar, with those in HuLys marginally longer. Hydrogen bonds between HuLys and lysozyme seen in both HuLys complexes are seen in all cases as well in the D1.3–lysozyme complex. This comparison of antibody–antigen contacts in the HuLys and D1.3 complexes was extended to include van der Waals interactions. The comparison showed three interactions in D1.3 closer than 4 Å, between Trp H52 and lysozyme Gly 117, which are not seen in HuLys. No interactions were found in both HuLys molecules that were not also seen in D1.3.

We interpret the shift of the HuLys antigen contacting residues from rough congruence to exact congruence with the cognate residues in D1.3 as evidence for a conformational correction mechanism that allows the antibody to attain precise stereochemical complementarity with antigen. The unliganded conformation of HuLys observed crystallographically (14) is unlikely to interact with the antigen as strongly as the conformation both HuLys and D1.3 adopt in the complex. During the antigen recognition process, the HuLys combining site must undergo a correction to the more favorable lysozyme binding conformation. Exactly such a mechanism was hypothesized in the initial report of humanizing the D1.3 heavy chain (36). X-ray data do not allow us to distinguish whether this involves an “induced fit” rearrangement of combining site residues after initial complex formation (37, 38) or isomerization of HuLys to the high affinity form before antigen encounter (39–41). D1.3 itself undergoes a small conformational change accompanying lysozyme complex formation (16), but this differs somewhat from the change in HuLys, as evidenced by the moderate disparity in D1.3 and HuLys unliganded conformations.

*Conformational Correction in Framework.* A second conformational correction mechanism appears to involve a subtle rearrangement of HuLys framework residues proximal to the CDRs. Evidence for this rearrangement is shown in Fig. 2. In 2 A, the framework of the Fv structure has been divided into layers according to CDR proximity. Residues within 4 Å of a CDR form the first layer, residues approaching between 4 and 8 Å the next layer, and so on. Fig. 2 C shows, for each layer, the degree of sequence identity between HuLys and cognate residues in the two parent antibody molecules. Here, HuLys and D1.3 have 100% sequence identity in the CDRs, whereas in all framework layers HuLys and the human molecules are more similar in primary structure. Fig. 2 B depicts a parameter more relevant to homology at the three-dimensional level. Here, the distance from each HuLys C $\alpha$  to the cognate C $\alpha$  in superposed D1.3, REI, or NEW molecules was determined. The difference between the HuLys to human and HuLys to mouse distance was then calculated, and the median for each residue layer was compiled. This difference is a measure of whether a particular layer of HuLys is generally more similar in conformation to D1.3 or to REI and NEW. We found that the CDRs of the mouse and humanized molecules are much more structurally similar than





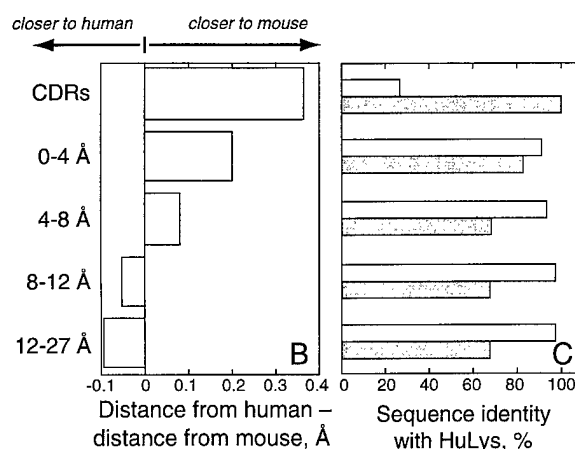


**Figure 2.** CDR-induced changes in framework conformation. (A) Cα trace of the HuLys Fv from molecule 1 of the HuLys-lysozyme complex crystal form, stereo view. Framework layers are colored according to CDR proximity. CDRs are colored red. Framework residues that have at least one nonhydrogen atom within 4 Å of any nonhydrogen CDR atom are colored maroon. Residues whose nearest atom to a CDR atom is within 4–8 Å are colored purple, within 8–12 Å colored green, and 12–27 Å colored black. (B) Conformational similarity between HuLys and D1.3 or HuLys and REI/NEW, by framework layer. Heavy and light chains of the mouse and human structures were independently superposed on HuLys molecules 1 and 2 using PDBFIT (33). The distance between cognate Cα atoms was calculated, and for each cognate set the value of the HuLys to D1.3 distance was subtracted from the HuLys to REI/NEW distance. The median difference for each framework layer is shown in the bar graph. A positive value indicates that the HuLys to human distance is greater than the HuLys to mouse distance for a majority of residues in that layer, and therefore that the HuLys structure is less similar to the human and more similar to the mouse structure for that layer. For these calculations we used a total of 112 CDR Cα atoms in the two crystallographically independent HuLys Fv molecules, 98 in the 0–4 Å layer, 88 in the 4–8 Å layer, 74 in the 8–12 Å layer, and 80 in the 12–27 Å layer. (C) Sequence identity between HuLys, D1.3, and REI/NEW, by framework layer. Open bars, HuLys compared to REI or NEW; filled bars, HuLys compared to D1.3. The humanized, mouse, and human protein sequences were aligned by Kabat residue number. The number of positions with identical residues in HuLys and D1.3 or HuLys and REI/NEW were then tabulated for each framework layer, and this value is presented in the figure as a percentage. The illustration was drawn using the program MOLSCRIPT (27).

lows humanizing to “work”. As a first approximation, mouse CDRs retain function on human frameworks because backbone conformations of hypervariable loops usually follow one of a small number of canonical structures regardless of chemical environment (42). Human frameworks can usually be found that will support a set of mouse CDRs identically to the mouse frameworks with which the CDRs were first isolated. In HuLys, we have identified a fine-tuning mechanism in which the mouse CDRs force nearby humanized framework residues toward the backbone conformation found in the corresponding D1.3 frameworks. The implication for humanizing is that although point mutations may have to be introduced into the frameworks to improve antigen binding by a humanized antibody, generally only a few are required, and these are necessary to recreate local structural motifs, such as the CDR-separating side chain at H71 (43). Finer-scale tailoring of framework structures

**Table 3.** rms Distances between Superimposed HuLys and Cα Atoms

HuLys	D1.3	Framework	CDR	Lysozyme
		Å	Å	Å
Liganded	Liganded	0.67	0.37	0.43
Free	Free	0.68	0.63	–
Liganded	Free	0.62	0.44	–

Distances were calculated between Cα atoms of each segment after superposition of those atoms. Each heavy chain and each light chain of the two HuLys molecules was superposed separately on the corresponding D1.3 chain. Each set of distances was separated into two lists, one containing framework residue distances and one containing CDR residue distances. Each entry in the Table was then calculated from the four (liganded) or two (free HuLys) corresponding lists of distances. Both liganded HuLys molecules in the crystallographic asymmetric unit were used in the calculation, but only one of the two free HuLys molecules was included because the CDRs of the heavy chain of the other are somewhat distorted by symmetry-related contacts. For lysozyme superpositions, the two lysozyme molecules of the HuLys complex were superposed on the D1.3 lysozyme. D1.3 structures used for comparison were obtained from the Brookhaven Protein Data Bank, and correspond to the accession numbers 1VFA (free Fv) and 1 VFB (Fv-lysozyme complex).

**Table 4.** Comparison of Hydrogen-bonded Antibody–Antigen Contact Distances in HuLys and D1.3

Fv atom	Lysozyme atom	D1.3 distance	HuLys distance (molecules 1,2)
		Å	Å
Ly30 His ND1	129 Leu OT2	3.4	3.3, 4.6
L50 Tyr OH	18 Asp OD1	3.2	3.2, 3.7
L50 Tyr OH	18 Asp OD2	2.7	2.7, 2.9
L53 Thr OG1	19 Asn ND2	2.8	3.2, 3.1
L91 Phe O	121 Gln NE2	2.8	3.0, 3.0
L93 Ser N	121 Gln OE1	2.9	2.9, 2.8
H53 Gly N	117 Gly O	2.8	3.1, 3.3
H96 Arg NH2	102 Gly O	2.7	2.8, 4.0
H97 Asp OD1	24 Ser OG	2.8	2.8, 3.2
H97 Asp OD1	27 Asn ND2	3.1	3.5, 3.1
H97 Asp OD2	22 Gly O	3.0	3.0, 3.0
H97 Asp OD2	24 Ser N	2.9	2.9, 3.0
H98 Tyr OH	119 Asp OD1	2.7	2.9, 2.7
H98 Tyr OH	120 Val N	3.2	3.3, 3.2
H98 Tyr OH	121 Gln N	3.0	3.2, 2.9
H99 Arg NH1	22 Gly O	2.8	3.0, 3.0
H99 Arg NH2	22 Gly O	3.4	2.7, 3.2

All direct D1.3-lysozyme hydrogen bonds shorter than 3.5 Å are listed. These residues are a subset of a larger list, which includes residues that hydrogen bond via water molecules.

appears unnecessary. At the combining site, the conformation of a humanized antibody free in solution may differ somewhat from that of the parent mouse antibody, as was found by comparing HuLys and D1.3 (14). However, a second conformational correction mechanism compensates for imprecisions in lock and key complementarity that would otherwise result from apposing rigid bodies. Interaction with antigen erases these differences by selecting or inducing a conformation of HuLys nearly identical to that in the D1.3-lysozyme complex. A concomitant shift towards the uncomplexed mouse antibody conformation occurs as well.

Lastly, 25 tightly ordered water molecules form a layer at the D1.3-lysozyme interface (35, 44, 45). These water molecules bridge many antibody-antigen contacts, are thermodynamically significant in the antigen-binding reaction, and many are conserved in free, complexed, and mutant D1.3 structures, and hence must be considered an intrinsic part of the combining site. Though we cannot identify ordered solvent in HuLys at 2.7-Å resolution, it would seem essential for antigen recognition that CDRs in a humanized antibody recreate a water network similar to that in the combining site of the parent mouse antibody.

We thank Steve Sheriff, Thomas B. Lavoie, and Greg Winter for suggestions on the manuscript.

We gratefully acknowledge financial support from the Arnold and Mabel Beckman Foundation and the Department of the Army Breast Cancer Research Program (grant DAMD 17-97-1-7124).

Address correspondence to Jefferson Foote, Division of Molecular Medicine, Fred Hutchinson Cancer Research Center, 1100 Fairview Ave. North, C3-168, PO Box 19024, Seattle, WA 98109-1024. Phone: 1-206-667-6720; Fax: 1-206-667-6524; E-mail: jfoote@fhcrc.org

Received for publication 7 October 1997 and in revised form 2 December 1997.

## References

1. Jones, P.T., P.H. Dear, J. Foote, M.S. Neuberger, and G. Winter. 1986. Replacing the complementarity-determining regions in a human antibody with those from a mouse. *Nature*. 321:522-525.
2. Morrison, S.L., M.J. Johnson, L.A. Herzenberg, and V.T. Oi. 1984. Chimeric human antibody molecules: mouse antigen-binding domains with human constant region domains. *Proc. Natl. Acad. Sci. USA*. 81:6851-6855.
3. Boulianne, G.L., N. Hozumi, and M.J. Shulman. 1984. Production of functional chimaeric mouse/human antibody. *Nature*. 312:643-646.
4. Neuberger, M.S., G.T. Williams, E.B. Mitchell, S.S. Jouhal, J.G. Flanagan, and T.H. Rabbitts. 1985. A hapten-specific chimaeric IgE antibody with human physiological effector function. *Nature*. 314:268-270.
5. Schaible, G., G.A. Rappold, W. Pargent, and H.G. Zachau. 1993. The immunoglobulin kappa locus: polymorphism and haplotypes of Caucasoid and non-Caucasoid individuals. *Hum. Genet.* 91:261-267.
6. Matsuda, F., E.K. Shin, H. Nagaoka, R. Matsumura, M. Haino, Y. Fukita, S. Taka-Ishi, T. Imai, J.H. Riley, R. Anand, E. Soeda, and T. Honjo. 1993. Structure and physical map of 64 variable segments in the 3' 0.8-megabase region of the human immunoglobulin heavy-chain locus. *Nat. Genet.* 3:88-94.
7. Cook, G.P., I.M. Tomlinson, G. Walter, H. Riethman, N.P. Carter, L. Buluwela, G. Winter, and T.H. Rabbitts. 1994. A map of the human immunoglobulin VH locus completed by analysis of the telomeric region of chromosome 14q. *Nat. Genet.* 7:162-168.
8. Sasso, E.H., J.H. Buckner, and L.A. Suzuki. 1995. Ethnic differences in polymorphism of an immunoglobulin VH3 gene. *J. Clin. Invest.* 96:1591-1600.
9. Milner, E.C.B. 1996. Organization of the human VH locus and rearrangement patterns of the VH3 gene family. In *Human B Cell Superantigens*. M. Zouali, editor. Springer, New York. 1-10.
10. Hale, G., M.J.S. Dyer, M.R. Clark, J.M. Phillips, R. Marcus, L. Riechmann, G. Winter, and H. Waldmann. 1988. Remission induction in non-Hodgkin lymphoma with reshaped human monoclonal antibody CAMPATH-1H. *Lancet*. 2:1394-1399.
11. Wu, T.T., and E.A. Kabat. 1970. An analysis of the sequences of the variable regions of Bence Jones proteins and myeloma light chains and their implications for antibody complementarity. *J. Exp. Med.* 132:211-250.
12. Kabat, E.A., and T.T. Wu. 1971. Attempts to locate complementarity-determining residues in the variable positions of light and heavy chains. *Ann. NY Acad. Sci.* 190:382-393.
13. Riechmann, L., M. Clark, H. Waldmann and G. Winter. 1988. Reshaping human antibodies for therapy. *Nature*. 332:323-327.
14. Holmes, M.A., and J. Foote. 1997. Structural consequences of humanizing an antibody. *J. Immunol.* 158:2192-2201.
15. Kabat, E.A., T.T. Wu, H.M. Perry, K.S. Gottesman, and K. Coeller. 1991. Sequences of Proteins of Immunological Interest. 5th ed. US Department of Health and Human Services, Public Health Service, National Institutes of Health, Bethesda.
16. Bhat, T.N., G.A. Bentley, T.O. Fischmann, G. Boulot, and R.J. Poljak. 1990. Small rearrangements in structures of Fv and Fab fragments of antibody D1.3 on antigen binding. *Nature*. 347:483-485.
17. Amit, A.G., R.A. Mariuzza, S.E.V. Phillips, and R.J. Poljak. 1986. Three-dimensional structure of an antigen-antibody complex at 2.8 Å resolution. *Science*. 233:747-753.
18. Poljak, R.J., L.M. Amzel, H.P. Avey, B.L. Chen, R.P. Phizackerly, and F. Saul. 1973. Three-dimensional structure of the Fab' fragment of a human immunoglobulin at 2.8 Å resolution. *Proc. Natl. Acad. Sci. USA*. 70:3305-3310.

19. Saul, F.A., and R.J. Poljak. 1992. Crystal structure of human immunoglobulin fragment Fab New refined at 2.0 Å resolution. *Proteins*. 14:363–371.
20. Epp, O., E.E. Lattman, M. Schiffer, R. Huber, and W. Palm. 1975. The molecular structure of a dimer composed of the variable portions of the Bence-Jones protein REI refined at 2.0 Å resolution. *Biochemistry*. 14:4943–4952.
21. Foote, J., and G. Winter. 1992. Antibody residues affecting conformation of the hypervariable loops. *J. Mol. Biol.* 224: 487–499.
22. Carter, P., R.F. Kelley, M.L. Rodrigues, B. Snedecor, M. Covarrubias, M.D. Velligan, W.L.T. Wong, A.M. Rowland, C.E. Kotts, M.E. Carver, et al. 1992. High level *Escherichia coli* expression and production of a bivalent humanized antibody fragment. *Bio/Technology* 10:163–167.
23. Neidhardt, F.C., P.L. Bloch, and D.F. Smith. 1974. Culture medium for enterobacteria. *J. Bacteriol.* 119:736–747.
24. Skerra, A., and A. Plückthun. 1988. Assembly of a functional immunoglobulin Fv fragment in *Escherichia coli*. *Science*. 240: 1038–1041.
25. Otwinowski, Z., and W. Minor. 1997. Processing of x-ray diffraction data collected in oscillation mode. *Methods Enzymol.* 276:307–326.
26. Navaza, J. 1994. AMoRe: an automated package for molecular replacement. *Acta Crystallogr. Sect. A. Found. Crystallogr.* 50:157–163.
27. Brünger, A.T. 1992. X-PLOR Manual, Version 3.1. Yale University Press, New Haven.
28. Brünger, A.T. 1992. Free R value: a novel statistical quantity for assessing the accuracy of crystal structures. *Nature*. 355: 472–475.
29. Kleywegt, G.J., and T.A. Jones. 1995. When freedom is given, liberties are taken. *Structure*. 3:535–540.
30. Tronrud, D.E., L.F. TenEyck, and B.W. Matthews. 1987. An efficient general-purpose least-squares refinement program for macromolecular structures. *Acta Crystallogr. Sect. A. Found. Crystallogr.* 42:489–501.
31. Laskowski, R.A., M.W. MacArthur, D.S. Moss, and J.M. Thornton. 1993. PROCHECK: a program to check the stereochemistry of protein structures. *J. Appl. Crystallogr.* 26: 283–291.
32. Milner-White, E.J., B.M. Ross, R. Ismail, K. Belhadj-Mostefa, and R. Poet. 1988. One type of gamma-turn, rather than the other gives rise to chain-reversal in proteins. *J. Mol. Biol.* 204:777–782.
33. McRae, D.E. 1992. A visual protein crystallographic software system for X11/Xview. *J. Mol. Graphics*. 10:44–46.
34. Padlan, E.A. 1994. Anatomy of the antibody molecule. *Mol. Immunol.* 31:169–217.
35. Bhat, T.N., G.A. Bentley, G. Boulot, M.I. Green, D. Tello, W. Dall'Acqua, H. Souchon, F.P. Schwarz, R.A. Mariuzza, and R.J. Poljak. 1994. Bound water molecules and conformational stabilization help mediate an antigen-antibody association. *Proc. Natl. Acad. Sci. USA*. 91:1089–1093.
36. Verhoeven, M.E., C. Milstein, and G. Winter. 1988. Reshaping human antibodies: grafting an antilysozyme activity. *Science*. 239:1534–1536.
37. Herron, J.N., X.M. He, D.W. Ballard, P.R. Blier, P.E. Pace, A.L.M. Bothwell, E.W. Voss, Jr., and A.B. Edmundson. 1991. An autoantibody to single-stranded DNA: comparison of the three-dimensional structures of the unliganded Fab and a deoxynucleotide-Fab complex. *Proteins*. 11:159–175.
38. Rini, J.M., U. Schulze-Gahmen, and I.A. Wilson. 1992. Structural evidence for induced fit as a mechanism for antibody-antigen recognition. *Science*. 255:959–965.
39. Lancet, D., and I. Pecht. 1976. Kinetic evidence for hapten-induced conformational transition in immunoglobulin MOPC 460. *Proc. Natl. Acad. Sci. USA*. 73:3548–3553.
40. Stevens, F.J., C.-H. Chang, and M. Schiffer. 1988. Dual conformations of an immunoglobulin light-chain dimer: heterogeneity of antigen specificity and idiotope profile may result from multiple variable-domain interaction mechanisms. *Proc. Natl. Acad. Sci. USA*. 85:6895–6899.
41. Foote, J., and C. Milstein. 1994. Conformational isomerism and the diversity of antibodies. *Proc. Natl. Acad. Sci. USA*. 91: 10370–10374.
42. Chothia, C., and A.M. Lesk. 1987. Canonical structures for the hypervariable regions of immunoglobulins. *J. Mol. Biol.* 96:901–917.
43. Tramontano, A., C. Chothia, and A.M. Lesk. 1990. Framework residue 71 is a major determinant of the position and conformation of the second hypervariable region in the VH domains of immunoglobulins. *J. Mol. Biol.* 215:175–182.
44. Braden, B.C., B.A. Fields, and R.J. Poljak. 1995. Conservation of water molecules in an antibody-antigen interaction. *J. Mol. Recognit.* 8:317–325.
45. Goldbaum, F.A., F.P. Schwarz, E. Eisenstein, A. Cauerhff, R.A. Mariuzza, and R.J. Poljak. 1996. The effect of water activity on the association constant and the enthalpy of reaction between lysozyme and the specific antibodies D1.3 and D44.1. *J. Mol. Recognit.* 9:6–12.
46. Kraulis, P.J. 1991. MOLSCRIPT: a program to produce both detailed and schematic plots of protein structures. *J. Appl. Crystallogr.* 24:946–950.